A&A 382, 241–255 (2002)
DOI: 10.1051/0004-6361:20011552

Astronomy & Astrophysics

Crystalline silicate dust around evolved stars⋆

III. A correlations study of crystalline silicate features

F. J. Molster[1,2,†], L. B. F. M. Waters[1,3], A. G. G. M. Tielens[4,5], C. Koike[6], and H. Chihara[7]

[1] Astronomical Institute "Anton Pannekoek", University of Amsterdam, Kruislaan 403, 1098 SJ Amsterdam, The Netherlands
[2] School of Materials Science and Engineering, Georgia Tech, Atlanta, GA 30332-0245, USA
[3] Instituut voor Sterrenkunde, Katholieke Universiteit Leuven, Celestijnenlaan 200B, 3001 Heverlee, Belgium
[4] SRON, PO Box 800, 9700 AV Groningen, The Netherlands
[5] Kapteyn Astronomical Institute, PO Box 800, 9700 AV Groningen, The Netherlands
[6] Kyoto Pharmaceutical University, Yamashina, Kyoto 607-8412, Japan
[7] Department of Earth and Space Science, Osaka University, Toyonaka 560-0043, Japan

Received 8 June 2001 / Accepted 5 November 2001

Abstract. We have carried out a quantitative trend analysis of the crystalline silicates observed in the ISO spectra of a sample of 14 stars with different evolutionary backgrounds. We have modeled the spectra using a simple dust radiative transfer model and have correlated the results with other known parameters. We confirm the abundance difference of the crystalline silicates in disk and in outflow sources, as found by Molster et al. (1999a). We found some evidence that the enstatite over forsterite abundance ratio differs, it is slightly higher in the outflow sources with respect to the disk sources. It is clear that more data is required to fully test this hypothesis. We show that the 69.0 micron feature, attributed to forsterite, may be a very suitable temperature indicator. We found that the enstatite is more abundant than forsterite in almost all sources. The temperature of the enstatite grains is about equal to that of the forsterite grains in the disk sources but slightly lower in the outflow sources. Crystalline silicates are on average colder than amorphous silicates. This may be due to the difference in Fe content of both materials. Finally we find an indication that the ratio of ortho to clino enstatite, which is about 1:1 in disk sources, shifts towards ortho enstatite in the high luminosity (outflow) sources.

Key words. infrared: stars – stars: AGB and post-AGB; mass loss – planetary nebulae – dust

1. Introduction

The Infrared Space Observatory (ISO) has provided a new and unprecedented view on the occurence and composition of circumstellar and interstellar dust. One of the surprises of the ISO mission was the discovery of ubiquitous crystalline silicates in circumstellar dust shells of both evolved and young stars (see e.g. Waters et al. 1996; Waelkens et al. 1996). We have carried out an extensive study of the presence and properties of crystalline silicates. The present study is the third in a series, in which we study these silicates using ISO spectra. In previous papers (Molster et al. 2002a; 2002b; hereafter Papers I and II respectively) we have measured and described the circumstellar dust features found in the infrared spectra of 17 stars with different evolutionary status. The majority of these features could be identified with crystalline olivines ($Mg_{2x}Fe_{2-2x}SiO_4$) and pyroxenes ($Mg_xFe_{1-x}SiO_3$), where $1 \geq x \geq 0$. Jäger et al. (1998, hereafter JMD) measured the mass absorption coefficient of crystalline pyroxenes and olivines with different Fe over Mg ratios. Bands of both materials show a shift in the wavelength position of the peaks to longer wavelengths with increasing Fe content. The detection of the 69 micron feature, which is very sensitive to the Fe/Mg ratio (Koike et al. 1993; JMD), as well as the relative strength of the crystalline silicate features in the spectrum of IRAS 09425-6040 (Molster et al. 1999a), led to the conclusion that the crystalline olivines observed in the ISO spectra are very Mg-rich ($x > 0.95$); the Mg-rich end member of the olivines is called forsterite.

Send offprint requests to: F. J. Molster,
e-mail: fmolster@so.estec.esa.nl
† *Present address:* ESA/ESTEC, RSSD-ST, Postbus 299, 2200 AG Noordwijk, The Netherlands

⋆ Based on observations with ISO, an ESA project with instruments funded by ESA Member States (especially the PI countries: France, Germany, The Netherlands and the UK) and with the participation of ISAS and NASA.

Similarly, the enstatite band at 40.5 μm is sensitive to the Mg/(Fe+Mg) ratio and points top the presence of Mg-rich pyroxenes. The identification of the dust species is very important for a better insight in the formation and evolution of dust. This may lead to a better understanding of the mass loss process and thus the evolution of the mass-losing star itself.

There is a clear separation between sources with and without a dusty disk. This difference is evident quantitatively in the sense that the crystalline silicate features are stronger with respect to the continuum in the sources which are surrounded by a disk (Molster et al. 1999a), and also qualitatively in the shape of the features, which is a proof for different dust properties (Paper I).

However, more quantitative statements are necessary to come to a better understanding of the nature of the circumstellar dust in these objects, and of their formation and processing history. In order to get these quantitative statements, a comparison with laboratory measurements is necessary. Unfortunately the laboratory measurements do not always agree with each other. In Paper II we discussed different laboratory measurements of olivines and pyroxenes, and possible causes of discrepancy. Despite these differences, qualitative agreement with the ISO spectra is already quite impressive as we will demonstrate in the present study.

In Sect. 2 we discuss trends in the position and width of the solid state bands. In Sect. 3 we apply a very simple optically thin dust model to the spectra to determine a typical temperature for the dust species. The results of this modelling are used to look for correlations which are discussed in Sect. 4.

Peak positions show variation from source to source. We adopt the naming in Paper I, which implies that if we refer to a wavelength position we use μm, while if we refer to the name of specific feature we will write "micron".

2. Peak positions and bandwidths

As the measurements in Paper I show, there is a spread in the peak positions and bandwidths of the different features (see e.g. Fig. 1, where we plotted the spread in the 2 strongest olivine peaks at 23.6 and 33.6 μm). There is no clear trend in the spread. We note that, apart from 89 Her, all disk sources show the 33.6 micron features at a longer wavelength than the outflow sources (see Fig. 1).

Here we will discuss possible causes for this spread. One of the best investigated causes for shifts in bands is the chemical composition. Difference in the mineralogical composition as well as the abundance of the different elements are known to change the peak positions. Another cause for a change in the peak position is the temperature: a lower temperature tends to narrow the features, shift them to shorter wavelengths and in some cases even split the band. A third method why bands shift and change width is variations in the size and shape of the dust grains. Changing the crystallinity of the material can also change

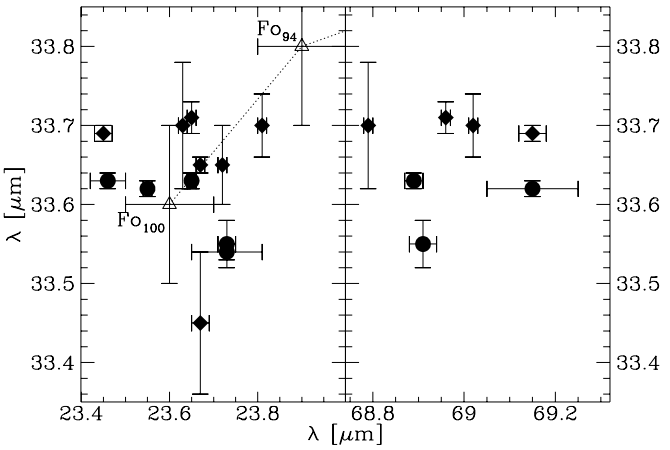

Fig. 1. The peak position of the forsterite peak at 23.7 μm versus the peak position of the forsterite peak at 33.6 μm (left side) and the forsterite peak position at 69.0 μm versus the position at 33.6 μm (right side). The diamonds denote the disk sources and the circles denote the outflow sources. The open triangles in the left part are room temperature laboratory observations for crystalline olivines with 0 and 6% of [FeO], Mg_2SiO_4 and $Mg_{1.88}Fe_{0.12}SiO_4$ respectively. In the right part the laboratory measurements fall off scale due to temperature effects (see Fig. 2 for these measurements). The error bars denote 1 σ errors in the wavelength position. No obvious correlations are visible.

the appearance of the feature. Below we will discuss these four effects more extensively.

2.1. Composition and temperature

JMD and Koike et al. (1993) showed that the inclusion of Fe in (crystalline) silicates will increase the wavelengths of the peak positions of the different features. Since the shift in wavenumbers is rather constant for the different features and proportional to the [FeO] content (JMD), these shifts are best seen for the features at the longest wavelengths (see Fig. 2). However, even a plot of the 69.0 micron feature versus the 33.6 micron feature does not show a clear trend (see Fig. 1). Both Figs. 1 and 2 show that the crystalline olivines are very Mg-rich and Fe-poor. The wavelength positions are consistent with an absence of Fe in these crystals. We conclude that the spread in the observations cannot (only) be explained by a very small and changing [FeO] content, therefore another mechanism should also be responsible.

Another mechanism to shift bands is the temperature. The 69.0 micron forsterite feature is found in different laboratory spectra where it always peaks at 69.7 μm, while in our ISO spectra it is always found around 69.0 μm. This shift is significant. Lowering the temperature will shift this feature bluewards (e.g. Bowey et al. 2000; Chihara et al. 2001). Another effect of a temperature decrease is a narrowing of this feature (see Fig. 2). This is a general property of crystalline features reflecting the anharmonic

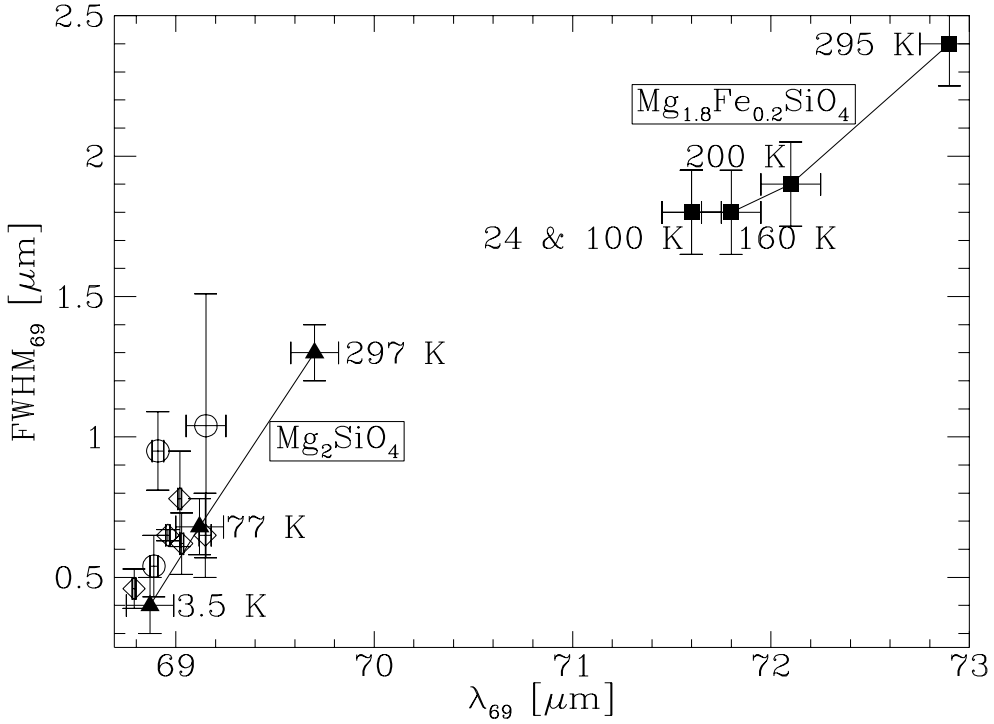

Fig. 2. The observed $FWHM$ and peak wavelength of the 69.0 micron feature in the spectra of the dust around stars (open diamonds for the sources with a disk and open circles for the sources without a disk) and in the laboratory at different temperatures (filled triangles – forsterite (Fo_{100}; Bowey et al. 2000), and filled squares – olivine (Fo_{90}; Mennella et al. 1998)). The temperatures are indicated at each point, and within the resolution the 24 K and 100 K for Fo_{90} are similar. Note that the measurements were not corrected for the instrumental $FWHM$ (≈0.29, for the ISO observations, and 0.25 and 1.0 μm for the laboratory observations of respectively Fo_{100} and Fo_{90}).

interaction of the phonon modes with the thermal phonon bath. At higher temperature the phonon modes are more excited and their distribution is broader. Hence, phonon-assisted absorption will shift bands redwards and will broaden their profiles at higher temperature. The amount of broadening depends on the origin of the feature. The 69.0 micron band is one of the best isolated bands in our spectrum to test for this effect. This narrowing of the absorption bands with decreasing temperature may be responsible for the fact that the observed band widths (of dust with typical temperatures of ≈100 K) in almost all cases is smaller than the laboratory widths measured at room temperature.

Besides shifting and narrowing a band, bands can also split in two components upon lowering the temperature (e.g. Bowey et al. 2000; Chihara et al. 2001). This might explain why in some sources we see a blend and in others we find two separate components. The narrowing (and splitting) of the features might provide an independent measurement of the temperature of the dust, without knowing anything of the rest of the spectrum!

We conclude from these comparisons that the crystalline silicates are very Mg-rich and cold. However, both processes shift the peaks together along the same line in the wavelength versus $FWHM$ diagram, so other processes must play a role too.

2.2. Shape and size

Strong transitions as found in the crystalline silicates can be very shape dependent. Not only the band strength is affected by grain shape, also the peak position can change dramatically. For instance, the peak wavelength of the 33.6 micron forsterite feature is located around 32.7 μm for spherical grains, while it shifts to 33.8 μm for a continous distribution of ellipsoids (see Fig. 3). The same figure also clearly demonstrates that the relative strength of the features is very shape dependent.

Another shape effect, which can play a role in the shape of the spectrum, is the preferential growth in the direction of 1 or 2 crystallographic axes (see e.g. Bradley et al. 1983 and reference in there). Although this is not likely to shift and broaden features that much, unless features corresponding to 2 different axes blend significantly, it does play a role in the relative strength of the features.

Difference in the size of the particles can also influence the spectra. However, this only becomes important when the size of the particles is comparable to the wavelength of the feature. Relatively large particles will broaden the feature and shift it to longer wavelengths.

Finally, we would like to note that coagulation and porousity can also have an effect on the width of the bands. This has been theoretically investigated for amorphous

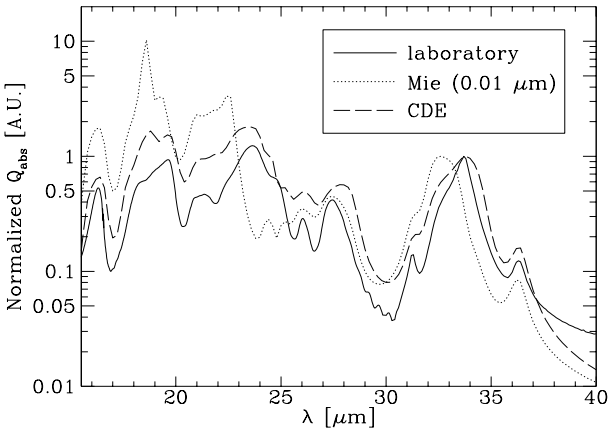

Fig. 3. The absorptivity ($Q_{\rm abs}$) of forsterite measured in the laboratory and calculated from the optical constants of Servoin & Piriou (1973) for spherical particles with a radius of 0.01 μm, using Mie calculations, and for a continuous distribution of ellipsoids (having a volume equal to that of a spherical particle with a radius of 0.01 μm). All curves are normalized to the peak value of the 33.6 micron feature. Note the difference in peak position and strength between the 2 different shape distributions.

quartz spheres by Bohren & Huffman (1983) and in the laboratory by Koike & Shibai (1994). This effect is difficult to quantify, but is likely to play a role for the crystalline silicates.

To conclude, we can say that shape effects might play a role in the spread of the peak positions.

2.3. Crystallinity

A final consideration should be the crystallinity, i.e. degree of lattice order or number density of lattice defects. Single crystals without defects show much sharper peaks than those with some defects. Therefore the width of the peaks might be an indication of the crystallinity of the dust grains.

Figure 4 shows a comparison between forsterite in different environments and 2 laboratory spectra. The forsterite measured by JMD was formed from a melt and probably polycrystalline, while the forsterite measured by Koike et al. (2000b) was a single crystal. The polycrystalline forsterite is expected to have defects where the different crystals meet each other.

The comparison with the astrophysical spectra suggests that around evolved stars nature produces nice single crystals, while around young stars poly-crystalline material seems to be formed. Around young stars it is expected that crystalline silicates form at the inner edge of accretion disks where the dust particles will (partially) melt. When mixed with cooler regions the liquid drops will likely solidify again and crystallize. In the outflows of evolved stars, gas will slowly cool and condense into dust grains. The time and temperature in these environments are likely to be sufficient to completely crystallize and get rid of all defects. It seems that this is not the case for young stars,

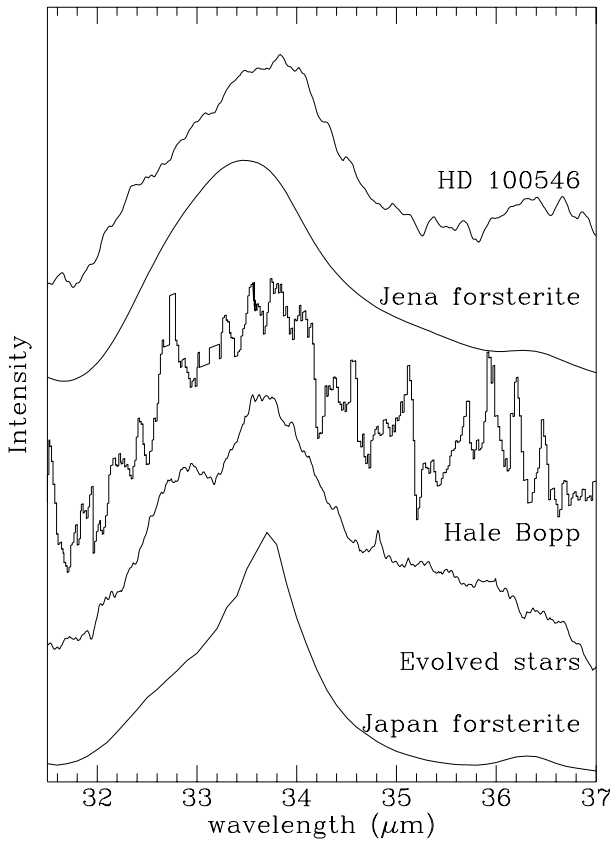

Fig. 4. The 33 micron complex of the young star HD 100546 (Malfait et al. 1998), the comet Hale Bopp (Crovisier et al. 1997) and an average of 33 micron complexes of evolved stars with evidence for a disk (Molster et al. submitted to A&A), together with 2 laboratory measurements of forsterite one done by JMD and one by Koike et al. (2000b). Note the difference in width of the 33.6 micron feature.

where the (partially) melted dust grains cool more rapidly, being unable to remove all the defects.

Figure 4 already shows that the crystallinity might shift the peak position of the feature a few tenth of a micron. So it is likely to play a role in the spread.

2.4. Summary

Above we discussed several mechanisms to shift and broaden features. We can conclude that the crystalline silicates are Fe-poor and cold. However, the reason for the spread in peak position is not well known. Shape effects and crystallinity, due to the different environments in which these particles are formed, are likely to play a role, but a combination with temperature and composition effects cannot be excluded.

Finally, it should be noted that all the features, of which the peak positions are plotted in Fig. 1 are part of a complex. Contributions of nearby features from other materials, which were not detected as separate features, might result in (apparent) differences of the peak positions. In this respect it is interesting to note that the 33.6 micron feature is the dominant feature in the

33 micron complex and also seems to show the least spread in the observations. The 23.6 and 69.0 micron features are part of the 23 and 60 micron complexes, respectively, and are much less dominant in these complexes. So relatively minor contributions will have less impact on the 33.6 micron feature than on the 23.6 and 69.0 micron features.

2.5. Other claimed trends

In a very limited sample Voors (1999) found a constant separation (in μm) between the 30.6 and the 32.8 micron band, which suggest a common species for these two features. We could not confirm this, but found a relation $\lambda_{32.8} = 0.8 \times \lambda_{30.6} + 8.39$ with λ_x indicating the wavelength of the x micron feature. Although we found a trend for those two features, we consider it unlikely that the 2 dust features come from the same material, since their strength normalized to the 33.6 micron feature does not correlate. Although we did not further investigate the correlation found, it may reflect a common cause, e.g. a difference in general temperature of the dust particles.

Based on a study of the crystalline silicate features in AFGL4106, Molster et al. (1999b) concluded that the forsterite features were broader than the enstatite features. We have tested whether this conclusion holds for our larger sample, using the mean results from Paper II, and could not confirm their claim. A similar negative result was found, when we compared the different laboratory datasets.

3. The modelling

In this section we will apply a simple dust emission model to derive the typical temperature and abundance ratio of forsterite and enstatite in the dust shells. We assume that the dust shell is optically thin at infrared wavelengths (which is reasonable because we see the dust features in emission), the grain size distribution of the different dust species is similar to what has been measured in the laboratory ($\ll 2$ μm, which also is quite realistic, because the width of the features indicates grains smaller than the wavelength) and that all grains of a given composition have the same (single) temperature (this is probably less realistic, but we only want to get a typical temperature for the dust species and are at the moment not interested in the temperature distribution). A comparison of several laboratory data sets with the observations indicates that the laboratory data of Koike et al. (2000b) give a good qualitative match to the observations. We will use this data set for our modelling. We determined an eye-ball spline-fit continuum, maximizing the continuum and still be smooth (no sudden changes in the slope), both in F_ν and F_λ. This continuum was derived in a similar way (using similar wavelength positions as continuum) for both the stellar and the laboratory spectra. Whenever possible we tried to use the whole wavelength range (SWS + LWS) to determine the placement of the continuum for the stellar spectra (see also Paper I). We have fitted the continuum subtracted spectra with the continuum subtracted forsterite and enstatite (50% ortho-enstatite and 50% clino-enstatite) mass absorption coefficients multiplied by blackbody functions.

$$F(\nu)_{\rm model} = \sum_i B(T_i, \nu) * \kappa(\nu)_i * M_i \quad (1)$$

$F(\nu)_{\rm model}$ is the calculated model flux, $B(T_i, \nu)$ is the blackbody function at temperature T_i of dust species i, $\kappa(\nu)_i$ is the mass absorption coefficient of dust species i and M_i is a multiplication factor which is related to the total mass of dust species i.

The temperature of the blackbody is not necessarily the same for enstatite and forsterite. In determining the best fit, we varied the temperature in steps of 5 K. The resulting spectra were separately scaled to fit the spectrum. This scaling factor is related to the mass of the dust species. The absolute masses requires knowledge of the distances to the stars but, for each source the masses of the different dust components can be directly compared. The mineral mass ratios determined in this paper assume that they have the same grain size and shape distribution (both around stars and in the laboratory samples). The best fits were determined by eye and no χ^2 method has been applied. This method is of sufficient accuracy given the current quality of the lab data and given the fact that several prominent dust features still lack identification, thus strongly affecting any χ^2 method. We found that the temperature and mass for forsterite could be determined using the 23 and 33 micron complexes, while the enstatite values are mainly based on the 28 and 40 micron features.

The results of this simple fitting procedure are shown in Figs. 5 to 16 and the derived temperatures and mass ratios are given in Table 1. We also derived an estimate for the typical temperature of the underlying continuum. For this we assumed that the continuum is caused by small grains with optical constants based on the amorphous silicate set 1 of Ossenkopf et al. (1992) and a continuous distribution of ellipsoids as shape distribution. We fitted the continuum to the original, not the continuum subtracted, spectra. An independent fit based on a $Q(\lambda) \sim \lambda^{-1}$ emissivity law gave similar temperatures. This gave us confidence that the continuum temperature is reasonably well determined in this way. It should be noted that other shape distributions (e.g. spheres) and other sets of optical constants of amorphous olivines can easily change the derived temperature by ± 20 K, more often to higher than to lower temperatures. From these fits we could in principle derive a relative mass, like in the case of enstatite and forsterite. Although the uncertainties in the (mass) absorption coefficients (due to shape, size and compositional differences) are systematic, the spread in values makes it very difficult to interpret them and to compare them with other observations. Therefore, we have not given an amorphous over crystalline silicate mass ratio. However, since the differences between the different datasets are systematic, trends can still be derived from these numbers. For the remainder of this paper we will take the

Table 1. The derived temperatures for forsterite $T_{\rm f}$, enstatite $T_{\rm e}$ and the amorphous silicates $T_{\rm a}$ from our model fits. Also the forsterite to enstatite ratio is given. The "-" denotes that it was not possible to derive a realistic value. † indicates that it is not really possible to fit the spectrum with a single temperature, The temperatures here are found by a fit to the short wavelength side of the spectrum. The typical error in the temperature of the crystalline silicates is 10 K, for the continuum temperature about 20 K, and in the mass ratio a factor 2. (P)PN = (proto-)planetary nebula, RSG = red supergiant.

Star	Type	$T_{\rm f}$	$T_{\rm e}$	$T_{\rm a}$	$\frac{M_{\rm e}}{M_{\rm f}}$
Disk sources					
IRAS 09425-6040	C-star with O-dust	85	100	145	1.2
NGC 6537	hot PN	75	65	80†	5.8
NGC 6302	hot PN	65	70	80†	1.0
MWC 922	PPN?, Herbig star?	90	100	140	2.7
AC Her	RV Tauri star	100	90	225†	5.0
HD 45677	Herbig star?	140	140	235†	5.3
89 Her	PPN	110	100	320†	5.0
MWC 300	PPN?	90	90?	145	1.4?
HD 44179	C-PPN with O-dust	135	135	120	4.0
Outflow sources					
HD 161796	PPN	105	80	100	11.4
HD 179821	post-RSG?	75	65	90	3.3
AFGL 4106	post-RSG	100	80	120	8.0
NML Cyg	RSG	150	-	180	-
IRC+10420	post-RSG	90	-	160	-

temperature derived by the fit with the Ossenkopf data set as the continuum temperature (Table 1), because these fits tend to produce the best fits. We compared the temperatures found in this study with those found by Molster et al. (1999b, 2001a), and we found a reasonable agreement. Difference in the temperatures found could often be described to the use of different laboratory data sets.

Our simple model, consisting of only two crystalline dust components and a single temperature for each dust component, fits most stars very well, see e.g. MWC 922 (Fig. 8). Still, it is clear that this simple model is not sufficient to explain all the features. The main discrepancies between our model fits and the ISO data lie at the wavelengths below 20 μm. We note that the three stars with a continuum temperature above 200 K all show crystalline silicates in emission in the 10 micron region. The temperature of the crystalline silicates has been determined based on bands at wavelengths longwards of 20 micron. These bands are dominated by cool dust, and the derived low temperatures (Table 1) are too low to explain the strength of the crystalline silicate bands in the 10 micron complex. A second, much warmer, component must be introduced to explain these 10 micron bands. Likely a temperature gradient is present in these sources. The discrepancies shortwards of 20 μm do not solely reflect the presence of a temperature gradient in these sources, but indicate that still other dust components must be present. The 18 micron complex is badly fitted. The modelled 19.5 micron feature (originating from both forsterite and enstatite) is often much too strong and the modelled 18.0 and 18.9 micron features are often too weak when compared to the ISO spectra. The too strong 19.5 micron feature might be a radiative transfer effect, since this feature is less of a problem in the full radiative transfer modelling (see e.g. Molster et al. 1999b, 2001a). This might indicate that our assumption of $\tau \ll 1$ is not correct at wavelengths around 19.5 μm. The poor fit of the 18.0 and 18.9 micron features suggests the presence of another dust component.

There is more evidence for the presence of an extra dust component. The 29.6 and 30.6 micron features also need extra emissivity, as is very clear in the spectra of NGC 6537 (Fig. 6) and of NGC 6302 (Fig. 7). In these two sources the 40.5 micron feature is not well fitted, suggesting that the same dust component which is responsible for the 29.6 and 30.6 micron features also has a peak around 40.5 μm. A possible candidate for this extra dust component is diopside ($MgCaSi_2O_6$), which peaks at the required wavelengths. However this material also produces strong peaks at other wavelengths, e.g. at 20.6, 25.1 and 32.1 μm, which are observed in the ISO data, but

often not as strong as expected. Therefore, the identification of the carrier of the 29.6 and 30.6 micron features remains open. It should be noted, that the temperature and relative mass of enstatite are estimated from the 28 and 40 micron complexes. Therefore a significant contribution of an unknown dust component to one (or both) of these 2 complexes can change the estimated temperature and abundance of enstatite.

The 33.0 micron feature is not well fitted, but this feature is likely to be influenced by instrumental behaviour (see Paper II). In the 35 micron plateau we clearly miss intensity around 34.8 μm in all sources. The predicted 69.0 micron feature is often too weak with respect to the ISO spectra (see e.g. Fig. 15). This may be an indication for the presence of colder dust, and thus for a temperature gradient, we will come back to this later.

Apart from all the features that are missing, we also have a problem with too much intensity predicted by our modelling around 27 μm. This excess is mainly due to enstatite, but also forsterite contributes slightly. We are still looking for an explanation of this phenomenon.

Finally, we did not attempt to fit the absorption profiles. As stated above we assumed the dust was optically thin. Also, no attempt was done to fit the carbon dust features, which are present in some sources.

3.1. The sample stars

Here we describe the model fits to the spectra of the individual stars, which where analyzed in Paper I. For a description of the individual stars in this sample we refer to Paper I. From this sample we rejected Roberts 22 and VY 2-2, because the ISO satellite was unfortunately offset when observing these two objects resulting in large flux jumps in the overall spectrum. This made it impossible to derive temperature estimates of the dust around these two stars. OH26.5+0.6 has also not been fitted, because below 30 μm it has an absorption spectrum (Sylvester et al. 1999), which could not be described with our simple model.

The main uncertainties in the model fits are due to uncertainties in the continuum subtraction. This leads to errors in the temperature of the order of 10 K and mass uncertainties of the order of a factor 2. We note that for our modelling we completely rely on the laboratory data input. This may result in systematic effects on our derived temperatures and masses.

3.1.1. IRAS 09425-6050

The fit to the spectrum of IRAS 09425-6040 is shown in Fig. 5. The model fit also produces a somewhat too strong 19.5 micron feature. It should be noted that the full radiative transfer calculations of Molster et al. (2001a) produces excellent fits to the 19.5 micron feature. The broad feature at 11 μm is due to SiC. This very simple model predicts no significant flux in the 10 micron complex due to crystalline silicates, which is consistent with its absence in the ISO spectrum.

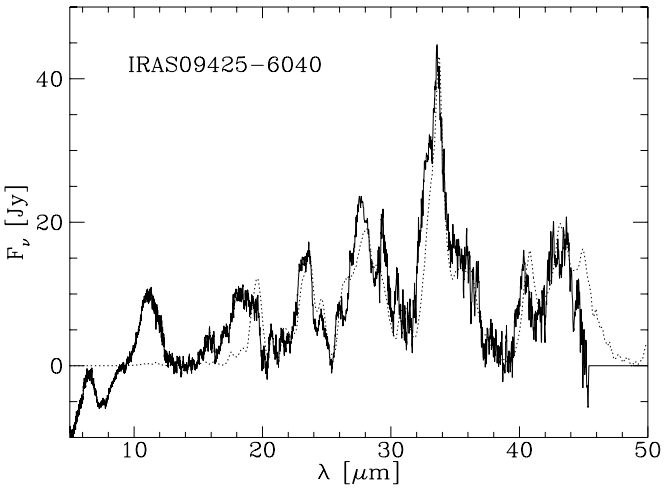

Fig. 5. A fit (dotted line) to the continuum subtracted spectrum (solid line) of IRAS 09425-6040. $T_{\rm f}$ = 85 K and $T_{\rm e}$ = 100 K.

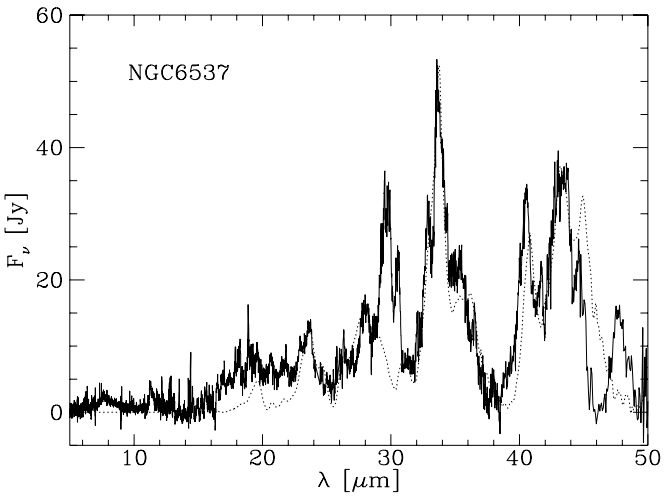

Fig. 6. A fit (dotted line) to the continuum subtracted spectrum (solid line) of NGC 6537. $T_{\rm f}$ = 75 K and $T_{\rm e}$ = 65 K.

The forsterite grains have a temperature of 85 K. This temperature agrees with the temperature range presented in the detailed radiative transfer model (Molster et al. 2001a). However, in contrast to the results presented here these detailed calculations predict that enstatite is much cooler than forsterite. As a result those models could not reproduce the relative strength of the observed 28 and 40 micron complexes. It also resulted in an unrealistically high mass for the enstatite. Molster et al. (2001a) argue that this might have to do with the not well known absorptivity of crystalline enstatite.

3.1.2. NGC 6537

The results for NGC 6537 are shown in Fig. 6. The temperatures found for the forsterite (75 K) and enstatite (65 K)

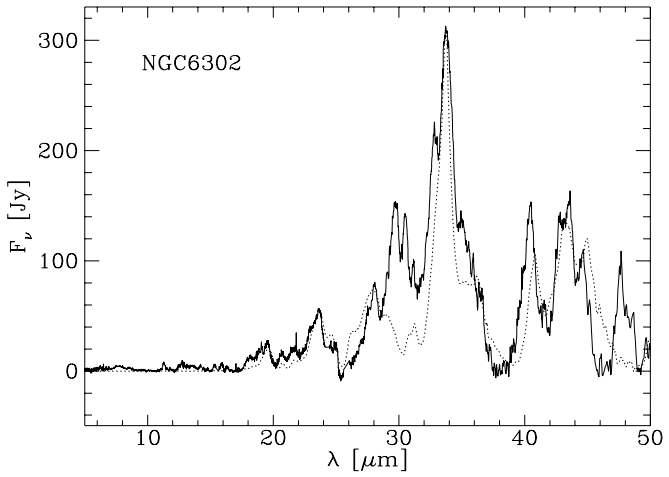

Fig. 7. A fit (dotted line) to the continuum subtracted spectrum (solid line) of NGC 6302. $T_{\rm f} = 65$ K and $T_{\rm e} = 70$ K.

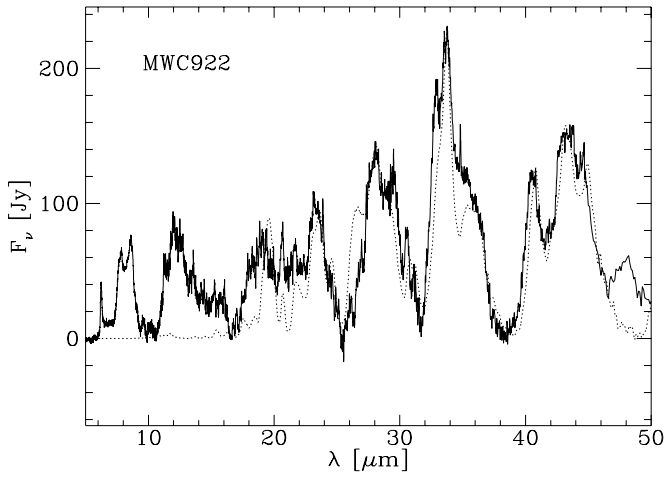

Fig. 8. A fit (dotted line) to the continuum subtracted spectrum (solid line) of MWC 922. $T_{\rm f} = 90$ K and $T_{\rm e} = 100$ K.

in NGC 6537 are among the lowest found in our sample. Note that if an extra dust component significantly contributes to the 40 micron complex, the temperature of enstatite will be higher (and its mass lower) than what has been determined here.

The spectral energy distribution of the complete spectrum is too broad to be fitted by a single temperature dust component.

3.1.3. NGC 6302

The continuum subtracted spectrum of NGC 6302 and its good fit are shown in Fig. 7.

Molster et al. (2001b) used the same method as used in this paper, and therefore found the same temperatures. As for NGC 6537, it was not possible to fit the spectral energy distribution with a single temperature dust component. Molster et al. (2001b) attribute the broad energy distribution to the presence of a population of large grains, which mainly contribute to the long wavelength side. The presence of this population of large grains is indicated by the gentle slope of the spectrum up to mm wavelengths (Hoare et al. 1992).

The temperature found for the enstatite and forsterite, respectively 65 and 70 K, are similar to the temperature of NGC 6537, which in many aspects looks very similar to NGC 6302. Kemper et al. (2001) assumed two temperature regimes: a cold one from 30 to 60 K, and a warm one from 100 to 118 K. Both components contain forsterite and enstatite. Our results, giving a temperature somewhere in between those two regimes, is in agreement with theirs, although the exact comparison is somewhat difficult.

3.1.4. MWC 922

The fit to the continuum subtracted spectrum of MWC 922 is one of the best we have (see Fig. 8). Especially the 40 micron complex is very well reproduced by our model, indicating that the 50% clino- and 50% ortho-enstatite are the right proportions for this object. At $\lambda < 16$ μm the spectrum of MWC 922 is dominated by PAH-features which were not incorporated in the fitting procedure.

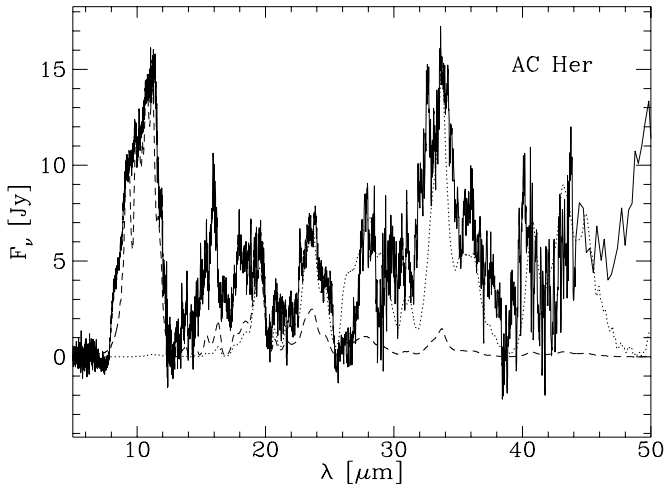

Fig. 9. A fit (dotted line) to the continuum subtracted spectrum (solid line) of AC Her. $T_{\rm f} = 100$ K and $T_{\rm e} = 90$ K (dotted line). The dashed line is a 700 K (for both forsterite and enstatite) model fit.

3.1.5. AC Her

A model with cool dust fits the long wavelength part (>20 μm) of the AC Her spectrum (dotted line in Fig. 9). However, the short wavelength features indicate the presence of a dust component with a much higher temperature. The temperature of this material is not well constrained. In Fig. 9 we show a fit of 700 K (dashed line in Fig. 9), but a similar fit could be derived with a temperature several hundreds degrees Kelvin higher or lower. Therefore it is impossible to give a reliable mass estimate for this hot component.

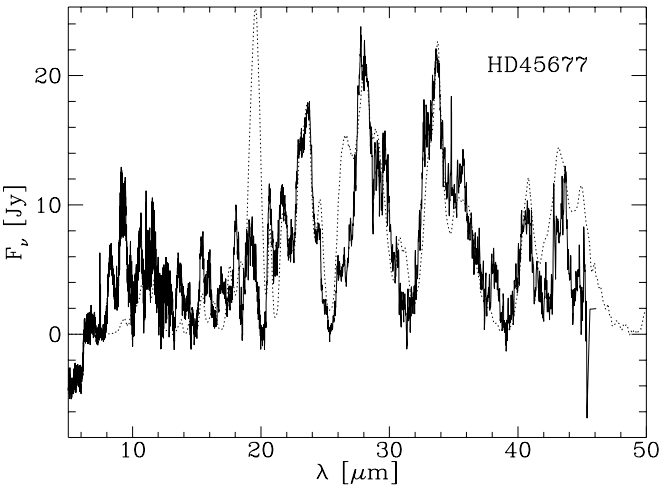

Fig. 10. A fit (dotted line) to the continuum and amorphous silicate subtracted spectrum (solid line) of HD 45677. $T_{\rm f} = 140$ K and $T_{\rm e} = 140$ K.

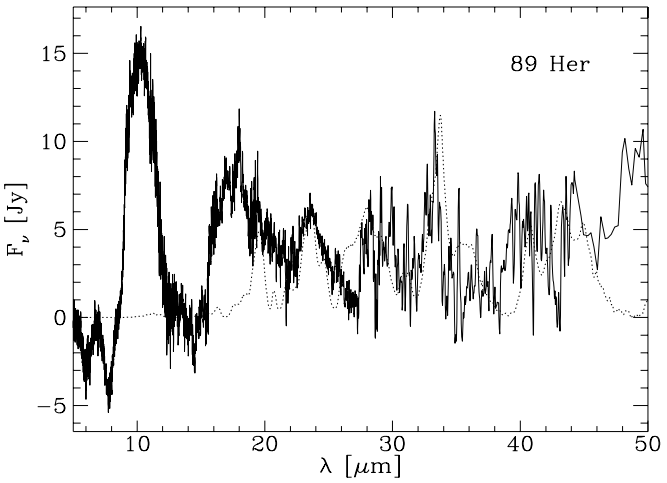

Fig. 11. A fit (dotted line) to the continuum subtracted spectrum (solid line) of 89 Her. $T_{\rm f} = 110$ K and $T_{\rm e} = 100$ K.

In our modelling we only assumed a single temperature. Based on the necessity of (at least) two different temperatures, the existence of a temperature gradient seems more likely. It is interesting to note that the overall spectrum of AC Her is very similar to that of comet Hale Bopp (Molster et al. 1999a) where we know that the dust is located in one place. Temperature differences found in the grains around this comet must therefore originate from the grain size differences. Small grains can account for the high temperature dust emission, while bigger grains are responsible for the low temperature dust emission. Such a scenario might also be possible for AC Her, which would imply that the dust might not have to be so close to the star as previously thought (e.g. Alcolea & Bujarrabal 1991). Jura et al. (2000) found a disk like structure for this object, which supports the above mentioned scenario. A full radiative transfer model fit would be necessary to completely understand the dust distribution around AC Her, but that is beyond the scope of this paper.

3.1.6. HD 45677

From the continuum subtracted spectrum of HD 45677 we first removed the broad amorphous silicate features (Fig. 10). We cannot exclude that we also removed part of the crystalline silicate features in the 18 micron complex in this way. This does not influence our results since these are mainly based on the 23, 28, 33 and 40 micron complexes. To fit the spectrum of HD 45677 we ignored the strength of the 19.5 micron feature, which is severely overestimated in our resulting fit. If we would have fitted the 19.5 and 40 micron features simultaneously, the 28 micron complex would have been severely underestimated. Likewise, attempts to fit the 18 and 28 micron complex together will result in a severely overestimated 40 micron complex, and also the fits to the 23 and 33 micron complexes will become worse. It is unlikely that this discrepancy can be fully explained by the subtraction of the amorphous silicates. Because this is not the only source with this problem, we leave this for future research.

Malfait (1999) also studied this star. He modelled this object with a radiative transfer code. HD 45677 could only be modelled with a 2 component dust shell, consisting of a hot shell, responsible for the main part of the flux up to 20 μm and a cool component which is the main contributor to the crystalline silicates features. Due to the method we use here, our temperature estimate is based on this cool component. Malfait finds a temperature between 250 and 50 K for this cool component. Unfortunately this is not specified for the different components separately, so we can only say that our temperature estimates do agree with this temperature range.

The predicted strength of the crystalline silicate features in the 10 micron complex is underestimated. Since the strength of the amorphous silicate band at 10 μm is uncertain, errors in the estimate of its contribution affect the strength of the crystalline silicate bands at these wavelengths and we did not attempt to fit the hot crystalline silicate compounds.

3.1.7. 89 Her

Before we fitted the continuum subtracted spectrum of 89 Her, we first subtracted a broad feature below the 26 to 45 μm region (Fig. 11). This feature is also seen in HD 44179 and probably AFGL 4106 and discussed in Paper II.

The continuum subtracted spectrum of 89 Her is quite noisy at the longer wavelengths, which makes the fits not as well constrained as in other stars. Also in this star warmer grains are necessary to explain the crystalline silicate structure found on top of the amorphous silicate feature in the 10 micron complex. Again, problems in the separation of the crystalline and amorphous silicates kept us from fitting this feature. Based on the CO observations and the near-IR excess, it was argued in Paper I, that

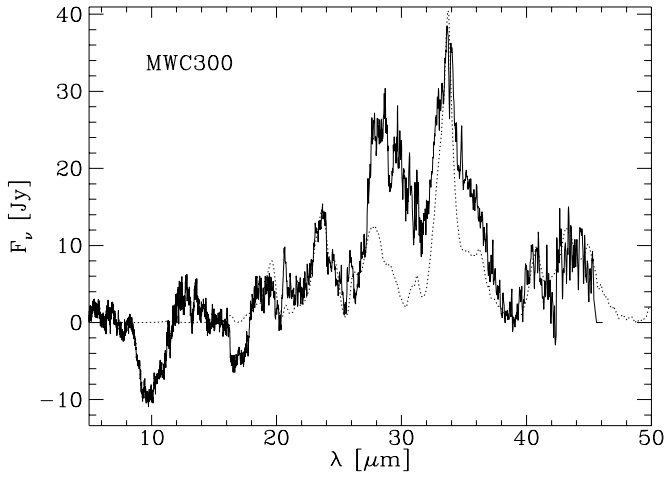

Fig. 12. A fit (dotted line) to the continuum subtracted spectrum (solid line) of MWC 300. $T_{\rm f} = 90$ K and $T_{\rm e} = 90$ K.

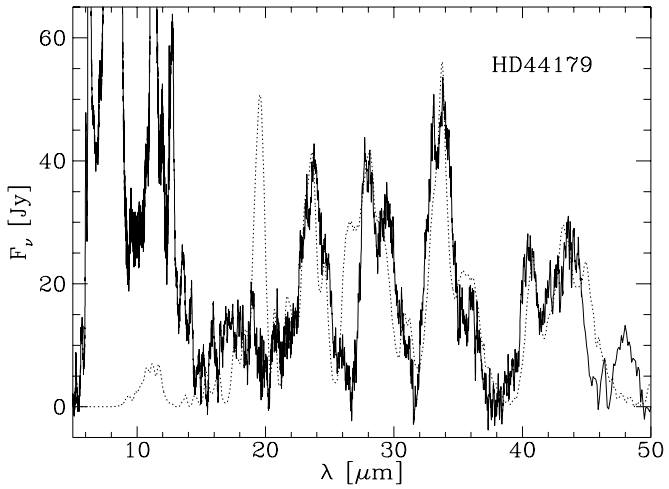

Fig. 13. A fit (dotted line) to the continuum subtracted spectrum (solid line) of HD 44179. $T_{\rm f} = 135$ K and $T_{\rm e} = 135$ K. Below 15 μm the spectrum is dominated by PAH features.

there must be dust with different temperatures, likely a temperature gradient, around 89 Her.

3.1.8. MWC 300

Although we have argued in this paper that the strength of the 19.5 micron feature is difficult to model correctly, we decided, because of the problems in the 28 micron complex to constrain the enstatite by the 19.5 micron feature in MWC 300 (see Fig. 12). If we would have fitted the strength of the 28 micron complex, and ignored the 19.5 micron feature, we would have derived a temperature of roughly 150 K, which is much larger than the forsterite temperature. It would also predict prominent features at the shorter wavelengths, which were not seen. The use of the 19.5 micron feature to constrain enstatite resulted in a similar temperature for the forsterite and enstatite dust species. This result, together with the reasonable fit at the 40 micron complex makes us confident in our approach for this star. We note however, that because of the problems with the 28 micron feature the values for enstatite are poorly constrained. The source of the extra flux in the 28 micron feature is unknown.

3.1.9. HD 44179

As for 89 Her, we removed the very broad feature in the 26 to 45 μm range in the continuum subtracted spectrum of HD 44179. The 18 micron complex seems to contain a contribution from amorphous silicates which was also removed. The result can be found in Fig. 13. It should be noted that a change in the subtraction of the broad 18 micron amorphous silicate feature, whose properties are not well determined, may change the derived temperature by more than the typical fitting error of 10 K.

The derived continuum temperature of 120 K is somewhat uncertain due to the complex nature of the source (Waters et al. 1998). Since the short wavelength part of the continuum is formed by C-rich grains, we based our fits on the long wavelength range. This will likely underestimate the temperature of the continuum. Taken all these uncertainties into account, the crystalline silicates may have an equal or even lower temperature than the amorphous silicates, as is found in the other stars.

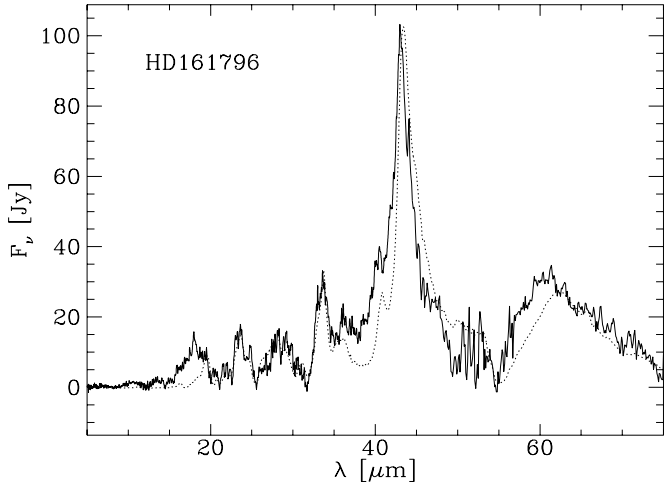

Fig. 14. A fit (dotted line) to the continuum subtracted spectrum (solid line) of HD 161796. $T_{\rm f} = 105$ K and $T_{\rm e} = 80$ K. We also included crystalline water ice with a temperature of 70 K.

3.1.10. HD 161796

The 40 micron complex in HD 161796 is dominated by crystalline water ice. In order to fit this spectrum (Fig. 14) we therefore added crystalline water ice to the spectrum (Smith et al. 1994). In general most features are reasonably well reproduced. The poor fit around 40 μm suggests that an underlying weak broad component contributes. Possibly, this is amorphous water ice.

Within the errors, the crystalline and amorphous temperatures are the same. The peak wavelength of the

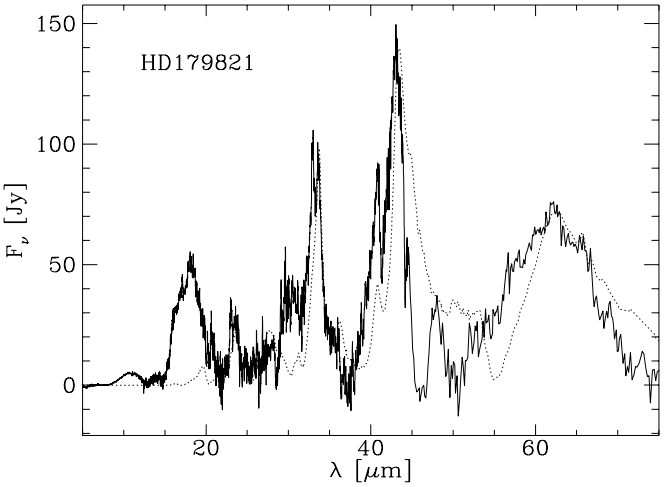

Fig. 15. A fit (dotted line) to the continuum subtracted spectrum (solid line) of HD 179821. $T_{\rm f}$ = 75 K and $T_{\rm e}$ = 65 K. To fit the 40 and 60 micron complex, we included crystalline water ice with a temperature of 45 K. Note, that we made no attempt to fit the amorphous silicate bands in the continuum subtracted spectrum.

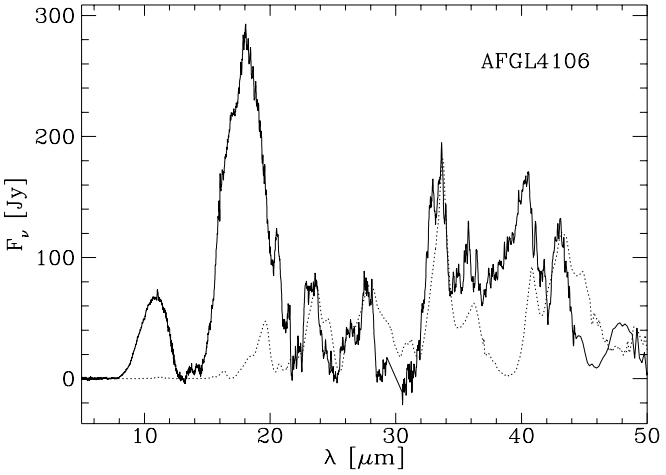

Fig. 16. A fit (dotted line) to the continuum subtracted spectrum (solid line) of AFGL 4106. $T_{\rm f}$ = 100 K and $T_{\rm e}$ = 80 K. Note, that we made no attempt to fit the amorphous silicate bands in the continuum subtracted spectrum.

crystalline water ice feature in our model is slightly offset from our ISO spectrum. This may be a temperature effect (Smith et al. 1994), reflecting the sensitivity of the emissivities to temperature.

3.1.11. HD 179821

HD 179821 shows prominent crystalline water ice features in the 40 and 60 micron complex. Therefore, we also added crystalline water ice in this model fit (Fig. 15). The crystalline silicate features are rather cold, 65 K for the enstatite and 75 K for the forsterite, therefore no detectable features are expected in the 10 micron region.

3.1.12. AFGL 4106

For the fit to the continuum subtracted spectrum of AFGL 4106 (Fig. 16) we changed the ratio of clino versus ortho enstatite to 1:3. Otherwise the 44.7 micron feature would have appeared too strong in the model spectrum. This feature is located in the wing of the 43.0 micron feature. The 43.0 micron feature is not well reproduced by our simple model, resulting in an offset of the 44.7 micron feature.

A broad feature between 30 and 45 μm seems present. It is not known whether this is the same feature as in 89 Her and HD 44179. It seems to peak at a longer wavelength (38 μm) than in the other two sources. Subtracting this feature, would increase both the temperature of forsterite and enstatite. The 40.5 μm feature is very strong, even if one removes this broad feature, indicating that other dust species are present. No attempt has been made to fit the substructure in the 18 micron band in view of the large and uncertain amorphous silicate contribution. In this star no detectable 10 micron structure is expected from the crystalline silicates, which is in agreement with the observations.

A full radiative transfer calculation was made for this source by Molster et al. (1999b). The enstatite abundance derived by them was based on the (wrong) assumption that the 32.8 micron feature was due to ortho-enstatite, and is therefore difficult to compare. They also used another dataset for forsterite, which has a different intrinsic strength ratio of the 23.7 and 33.6 micron features. This results in a lower temperature for forsterite in their calculations.

3.1.13. NML Cyg

We could not reliably fit enstatite to the spectrum of NML Cyg since a part of the 28 micron complex was missing, due to problems with the data reduction (see Paper I). We were able to fit forsterite to the continuum subtracted spectrum and found a temperature of about 150 K (not shown).

3.1.14. IRC+10420

Also for IRC+10420 we only fitted the forsterite component which appeared to be about 90 K (not shown). Enstatite could not be fitted due to the lack of data in the 28 micron region. We checked the 40 micron complex and, if enstatite would have been fitted, an ortho-enstatite to clino-enstatite ratio of 2:1 would probably give the best fit to the strength of the 44.7 micron feature.

4. Correlations

From the modelling, we were able to derive values for the temperature and the relative contributions to the total amount of dust mass by forsterite and enstatite. Correlating these values can give interesting insight in

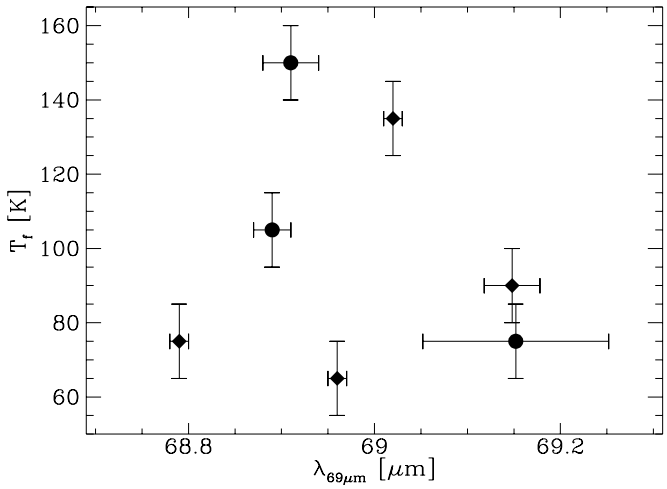

Fig. 17. The temperature of the forsterite grains versus the wavelength position of the 69 micron band. The circles are outflow sources and the diamonds are disk sources.

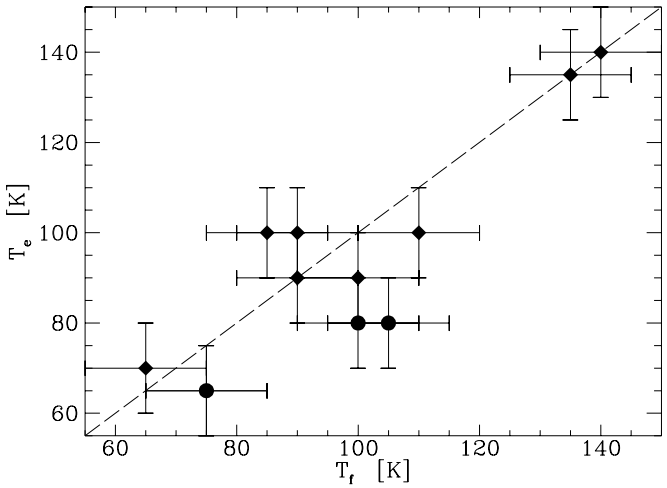

Fig. 18. The temperature of the forsterite grains versus the temperature of the enstatite grains. The diamonds are the disk and the circles are the outflow sources. The dashed line represents equal temperatures for the forsterite and enstatite grains. The errors are typically in the order of 10 K.

the dust inventory as we will show in this section. Since in Papers I and II it was found that there is a significant difference between the spectra of disk and of outflow sources, we will separate them. In all plots in this section the outflow sources are represented by a circle while the disk sources are represented by diamonds.

4.1. Temperature dependence of laboratory spectra: Peak width and position

In Sect. 2.1 we showed a relation between the peak position and FWHM of the 69 micron forsterite band and the temperature of the forsterite grains. Since we have now determined the temperature of the forsterite grains, we checked this relation in our data (Fig. 17). There is no clear correlation between these two quantities. A possible explanation for this scatter behaviour might be the fact that the temperature of the forsterite is determined from bands in the 20 to 40 μm range. The strength and width of the 69 micron feature may be dominated by much cooler dust. The predicted strength from our simple model fits, which is lower than the strength in our ISO spectra (see e.g. HD 179821), supports this statement.

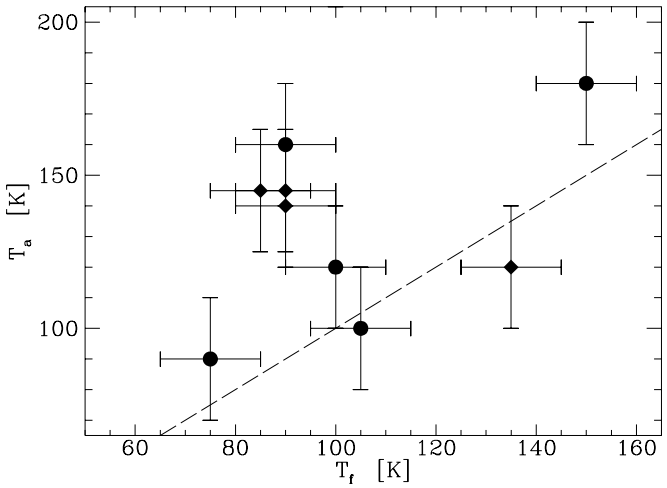

Fig. 19. The temperature of the forsterite grains versus the temperature of the amorphous silicate grains. The dashed line represents equal temperatures for the forsterite and amorphous silicate grains. The diamonds correspond to the disk sources, while the circles correspond to the outflow sources.

4.2. Other temperature trends

In Fig. 18 we compare the temperature of the enstatite and forsterite, derived from our simple model fits. For the disk sources the enstatite and forsterite grains seem to have an equal temperature, while in the 3 outflow sources the forsterite seems warmer.

In Fig. 19 we compare the forsterite temperature and the amorphous silicate temperature. We first note that, in general, the crystalline forsterite grains are colder than the underlying continuum consisting of amorphous silicates. The difference in temperature between the amorphous and crystalline silicates has probably to do with the difference in chemical structure. The crystalline silicates are Mg-rich (see this paper and Paper II), while the amorphous silicates must contain metals to explain their higher near-infrared absorptivity. Possibly the reaction of the Mg-rich crystalline silicates with gaseous iron may proceed in these outflows at temperatures well below the glass temperature leading simultaneously to amorphous and dirty silicates (Tielens et al. 1998).

For some stars like IRC+10420, MWC 922 and IRAS 09425-6040 the difference in temperature excludes the possibility of one grain population, which is partially crystalline. The crystalline and amorphous silicates must form two separate grain populations, which are not in thermal contact. From this simple model we cannot say

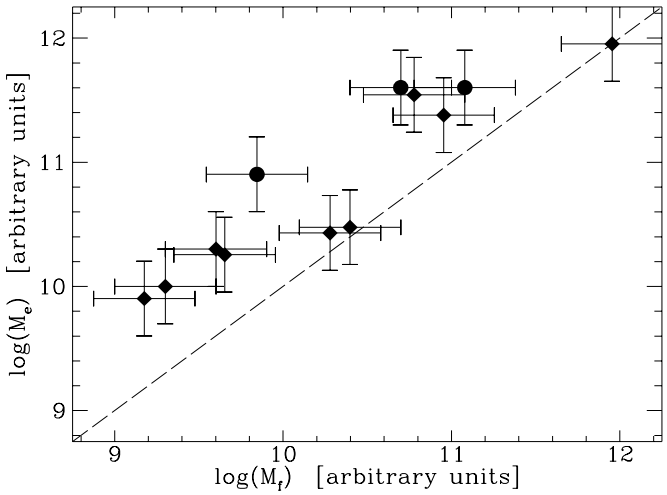

Fig. 20. The mass of the forsterite grains versus the mass of the enstatite grains. We have assumed that they have the same size and shape distribution. The dashed line represents equal masses for the forsterite and enstatite grains. The outflow sources are marked as a circle while the disk sources are marked with a diamond.

that they are also spatially separated, but radiative transfer modelling (Molster et al. 1999b, 2001a) indicates that this is not necessary. Finally, we note that there is no obvious separation between the disk and the outflow sources. Because of the analogy between the different sources, we expect that this grain segregation is valid for all sources in our sample.

4.3. Abundance trends

From our modelling we were also able to derive an abundance ratio for enstatite and forsterite (Fig. 20). In all sources, except NGC 6302, the enstatite is more abundant than the forsterite, on average a factor 3–4. Again there seems to be a difference between the disk and outflow sources. The outflow sources have, on average, a higher enstatite over forsterite ratio than the disk sources. We note however, that the number of outflow sources is low and more data is required to confirm this trend.

If crystallization of the amorphous grains is a thermally driven process, it is expected that warmer dust shells would show a higher crystalline silicate fraction. This effect would be most clear in the disks sources, where the dust stays at roughly the same place. In the outflow sources, the temperature of the optically thin dust shell is more an indication of the age of the dust. Cooler dust would be further out and therefore older, in which case an increase of the crystallinity with a lowering of the temperature may even be possible. We investigated the crystalline over amorphous silicates abundance ratio with the temperature of the amorphous silicates. We excluded AC Her, 89 Her and HD 45677 from this analysis because the continuum and feature temperatures derived likely do not reflect particles with the same size distribution and/or location around these objects, resulting in unrealistic mass ratios. No clear relation could be found between the temperature of the amorphous silicates versus the crystallinity, neither for the disk nor for the outflow sources. The crystallization process is either a relic of the past or it is not thermally driven. This is not too surprising. Thermally driven crystallization requires temperatures of ≈1000 K (Hallenbeck & Nuth 1998), which is well above the temperature of either the crystalline or amorphous silicates in our sources.

4.4. Crystallinity versus stellar flux ratio

It has been suggested by Waters et al. (1999) that the enstatite over forsterite ratio increases with luminosity of the star. They based their conclusions on the ratio of the 32.97 and 33.6 micron bands. They attributed the former band to enstatite, and the latter one to forsterite. Unfortunately, the 32.97 micron band is strongly affected by instrumental effects (see Paper II), which are most prominent in the brightest sources. These are usually also the intrinsic most luminous sources, such as IRC+10420 and NML Cyg. Since it is likely that in high flux sources grain formation will result in different ratios of the dust species we still decided to investigated this scenario. We could find no trend for the stars in our sample, which had a reliable distance (and thus flux) estimate.

5. Discussion

Most features can be explained with forsterite and enstatite. However laboratory spectra of these species often produce too broad bands. Most laboratory spectra were measured at room temperature, while the dust species around our stars are in the order of 80 K. Lowering the temperature can narrow the dust features, and this might be the natural solution for the width problem. It can also solve another problem. The 69.0 micron feature has been attributed to forsterite. It is very sensitive to the Fe/(Mg+Fe) ratio in olivine, and one of the key features for the determination of the Fe content in crystalline silicates. However in most lab spectra it peaks at 69.7 μm. Recent laboratory measurements show that this feature shifts to shorter wavelengths when the sample is cooled and will be at ≈69.1 μm at 77 K and even at ≈68.8 μm when measured at 4 K (Bowey et al. 2000). At the same time, the feature narrows (cf. Fig 2). So it seems that the temperature dependence is able to solve also this problem.

From the correlation study in this chapter a clear difference between the disk and the outflow sources emerges. The differences found in Papers I and II were based on the shape and strength of the different solid state features in the spectrum. These differences can now be traced back to differences in temperature and chemical composition of the circumstellar dust. The outflow sources seem more abundant in cold enstatite grains than the disk sources, although more observations would help to quantify this better. There are also indications that in the high luminosity outflow sources the ortho- over clino-enstatite

abundance ratio is larger than unity (see AFGL 4106 and IRC+10420), while in the other (disk) sources nice fits were obtained with a ratio of unity. Because of the large crystalline water-ice component in the 40 micron complex of HD 161796, it is difficult to quantify its ortho- over clino-enstatite ratio. Therefore we cannot exclude that this difference we see is related to the more massive nature of the central stars of AFGL 4106 and IRC+10420 rather than the disk-outflow character. The difference between the disk and the outflow sources might be related to differences in conditions during the condensation of the grains out of the hot gas, and/or to differences in the conditions since the formation of the dust particles. Smyth (1974) found that clino-enstatite slowely inverts to ortho-enstatite between 920 and 1220 K. Dust particles will stay longer within this temperature range in the case of massive stars than for low mass stars. This might explain the overabundance of ortho-enstatite in IRC+10420 and AFGL 4106 with respect to the other stars. Another possible difference during the formation of these grains could be the amount of radiation pressure exerted on the particles. It is expected to be lower in the disk sources, otherwise the disk is likely to be blown away. Also the presence of a companion – most if not all disk sources are a binary system – might influence the dust forming process. If, on the other hand, we assume that the initial (forming) conditions are similar for the disk and outflow sources, than the differences in the conditions after formation must be dominant. Time is an obvious differences. Also a relation with grain coagulation – the disks contain large grains – cannot completely be ruled out.

We note that clino-enstatite is often found in meteorites on earth. The process responsible for the overabundance of clino-enstatite in meteorites in the disks of young stars might be the same as the one in the disks around evolved stars. We also want to note that in chondrites or primitive meteorites, i.e the less processed ones, clino-pyroxenes are less abundant than the ortho-pyroxenes. This similarity between the disks around young and around evolved stars, is new evidence to the hypothesis that the circumstances and processes in disks around young stars are very similar to these in disks around evolved stars, although their origin is quite different.

The equal temperature of enstatite and forsterite in the disk sources, is in principle compatible with the assumption that enstatite and forsterite are present as a composite grain in the disk sources. However, it is equally well possible that their individual equilibrium temperatures are similar, in which case they can still be individual grains. New uninterupted laboratory measurements of the optical properties of both materials, especially in the wavelength range where they absorb the stellar light and emit the thermal radiation, would allow us to make these kind of calculations and settle this point. The different temperatures found for forsterite and enstatite in the outflow sources suggests two separate grain populations in these environments.

6. Conclusions

We can summarize the main results of this study as follows:

1 The ISO spectra could be reasonably well fitted with laboratory spectra of forsterite and enstatite.
2 The models underestimate the flux at 18, 29.6, 30.6, 48 μm and sometimes at 40.5 μm, which is an indication for the presence of (an)other dust component(s). No convincing identification could be made yet. Diopside does have features at most of these wavelengths, but also strong features at others which are weak or absent in the ISO-spectra.
3 The 19.5 micron feature is often overestimated by our model spectra. No explanation is yet known for this phenomenon, but it should be noted that in the full radiative transfer modelling it appeared to be much less of a problem. This might indicate that optical depth effects play a role. Also the calculation of the absorption coefficients from the constants instead of the absorption coefficients from laboratory particles might lead to differences.
4 The band width of the laboratory data is larger than in our ISO spectra. This difference is likely a temperature effect, and might be used as an independent temperature indicator. Especially the 69.0 micron band is very suitable for this analysis.
5 The temperature of the forsterite and enstatite grains are (almost) similar for the disk sources, while the forsterite is slightly warmer in the outflow sources. This would imply that the forsterite and/or enstatite grains differ slightly in the disk and outflow sources. It is not clear whether this difference is due to a different formation process, or due to a different dust process history after the grain formation. Since this trend is only based on 3 sources more data is required to confirm the difference between the dust and outflow sources.
6 The crystalline silicates are colder than the amorphous silicates. This is probably due to the difference in chemical composition. No Fe is present in the crystalline silicates, while in the amorphous silicates it is expected to explain the higher absorptivity. This difference in temperature also implies that the crystalline and amorphous grains are two distinct grain populations.
7 Enstatite is on average a factor 3–4 more abundant than forsterite in our sources. There are indications that the enstatite over forsterite ratio in the outflow sources is higher than in the disk sources.
8 In the low luminosity sources the spectra were well fitted with an equal amount of ortho- and clino-enstatite, while in the two high luminosity sources more ortho-enstatite seems to be present.
9 No correlation could be found between the crystallinity and the temperature of the dust. Also the luminosity of the stars does not seem to be correlated with the enstatite over forsterite ratio.

10 These simple model fits already give a good insight in the dust around our stars. In Paper I the shape of the features naturally separated the disk and outflow sources. In this study the differences between these two categories became again evident.

Acknowledgements. We greatly thank Janet Bowey for providing her laboratory data. FJM wants to acknowledge the support from NWO under grant 781-71-052 and under the Talent fellowship programm. LBFMW acknowledges financial support from an NWO "Pionier" grant.

References

Alcolea, J., & Bujarrabal, V. 1991, A&A, 245, 499
Bohren, C. F., & Huffman, D. R. 1983, Absorption and scattering of light by small particles (John Wiley and Sons Inc., New York)
Bowey, J. E., Lee, C., Tucker, C., et al. 2000, in ISO beyond the peak, ed. A. Salama, ESA SP-456, 339
Bradley, J. P., Brownlee, D. E., & Veblen, D. R. 1983, Nature, 301, 473
Chihara, H., Koike, C., & Tsuchiyama, A. 2001, PASJ, 53, 243
Crovisier, J., Leech, K., Bockelee-Morvan, D., et al. 1997, Science, 275, 1904
Cohen, M., Barlow, M. J., Sylvester, R. J., et al. 1999, ApJ, 513, L135
Hallenbeck, S., & Nuth, J. 1998, A&SS, 255,427
Hoare, M., Roche, P. F., & Clegg, R. E. S. 1992, MNRAS, 258, 257
Jäger, C., Molster, F. J., Dorschner, J., et al. 1998, A&A, 339, 904 (JMD)
Jura, M., Chen, C., & Werner, M. W. 2000, ApJ, 541, 264
Kemper, F., Jäger, C., Waters, L. B. F. M., et al. 2001, submitted to Nature
Koike, C., Shibai, H., & Tuchiyama, A. 1993, MNRAS, 264, 654
Koike, C., & Shibai, H. 1994, MNRAS, 269, 1011
Koike, C., & Shibai, H. 1998, ISAS Report, No. 671
Koike, C., Tsuchiyama, A., Shibai, H., et al. 2000a, A&A, 363, 1115
Koike, C., Chihara, H., Tsuchiyama, A., et al. 2000b, in Proceedings of the 33rd ISAS Lunar and Planetary Symposium, 95
Malfait, K., Waelkens, C., & Waters, L. B. F. M. 1998, A&A, 332, L25
Malfait, K. 1999, Ph.D. Thesis, Catholic University Leuven
Mennella, V., Brucato, J. R., Colangeli, L., et al. 1998, ApJ, 496, 1058
Molster, F. J., Yamamura, I., Waters, L. B. F. M., et al. 1999a, Nature, 401, 563
Molster, F. J., Waters, L. B. F. M., Trams, N., et al. 1999b, A&A, 350, 163
Molster, F. J., Yamamura, I., Waters, L. B. F. M., et al. 2001a, A&A, 366, 923
Molster, F. J., Lim, T. L., Sylvester, R. J., et al. 2001b, A&A, 372, 165
Molster, F. J., Waters, L. B. F. M., Tielens, A. G. G. M., & Barlow, M. J. 2002a, A&A, 382, 184 (Paper I)
Molster, F. J., Waters, L. B. F. M., & Tielens, A. G. G. M. 2002b, A&A, 382, 222 (Paper II)
Ossenkopf, V., Henning, Th., & Mathis, J. S. 1992, A&A, 261, 567
Servoin, J. L., & Piriou, B. 1973, Phys. Stat. Sol. (B), 55, 677
Smith, R. G., Robinson, G., Hyland, A. R., & Carpenter, G. L. 1994, MNRAS, 271, 481
Smyth, J. R. 1974, Amer. Mineral., 59, 345
Sylvester, R. J., Kemper, F., Barlow, M. J., et al. 1999, A&A, 352, 587
Tielens, A. G. G. M., Waters, L. B. F. M., Molster, F. J., & Justtanont, K. 1998, ApSS, 255, 415
Voors, R. H. M. 1999, Ph.D. Thesis, University of Utrecht
Waelkens, C., Waters, L. B. F. M., de Graauw, M. S., et al. 1996, A&A, 315, L245
Waters, L. B. F. M., Molster, F. J., de Jong, T., et al. 1996, A&A, 315, L361
Waters, L. B. F. M., Waelkens, C., van Winckel, H., et al. 1998, Nature, 391, 868
Waters, L. B. F. M., Molster, F. J., & Waelkens, C. 1999, Asymptotic Giant Branch Stars, ed. T. Le Bertre, A. Lèbre, & C. Waelkens, IAU Conf. 191, 209